
Chapter II

Theoretical Background

Chapter II

THEORETICAL BACKGROUND

2.1	Introduction	
2.2	Methods of thin film preparations	
2.3	Characterization techniques	
	2.3.1	X-ray diffraction
	2.3.2	Scanning electron microscopy
	2.3.3	Energy dispersive X-ray analysis (EDAX)
	2.3.4	Optical absorption and transmission
	2.3.5	Electrical resistivity
	References	

CHAPTER II

THEORETICAL BACKGROUND

2.1 Introduction

Thin film is defined as any solid or liquid system which possesses at most two-dimensional order or periodicity. Properties of thin film differ significantly from those of bulk due to surface and interface effects; this dominates overall behavior of the thin films. The common factor in thin film deposition is that they are atomistic in nature i.e. films are grown atom-by-atom. Thin films are of increasing interest owing to their numerous applications in all kinds of scientific, industrial and technological applications. The advantage of thin film devices are low material consumption and possible use of flexible substrates [1]. For this reason, there are always growing and urgent needs to find new, economical and simple techniques to prepare thin films. Also, a specific need appears for methods of preparation of thin films with large areas used in photovoltaic applications. To respond to this need, several research groups have worked in recent years on the preparation and characterization of the thin oxide films [2, 3]. Thin film plays an important role in the present day technology development; and techniques of the thin film deposition after a major key to the fabrication of solid state microelectronic devices. There are various methods of preparation of thin films. Out of which spray pyrolysis is of great importance due to its low cost. It is simple, easy, safe to use and can be used for large area deposition.

This chapter describes the various methods of thin film preparation and various characterization techniques used to study the properties of thin films. The semiconducting material, in thin film form are of particular interest of photovoltaic devices, transparent electrodes, surface acoustic wave devices, low emissive coating for architectural glass,

solar front panel display, various gas sensors, and heat reflectors for advanced gazing in solar applications. The experimental details pertain to the evaluation of various properties using analytical techniques viz. X-ray diffraction (XRD), scanning electron microscopy, optical transmission and electrical resistivity measurement.

2.2 Methods of thin film preparation

In general, many thin film deposition techniques have one common element i.e. they are atomistic in character. In other words, they are grown one atom at a time. This enables the researchers to create thin film systems, which could not ordinarily be expected to be possible. To be able to fully exploit this, one requires good knowledge and appreciation of surface process as well as nucleation, growth and morphology of evolving films. Thin film deposition is broadly classified as physical and chemical methods [4,5]. Physical methods include vacuum evaporation and sputtering, where the deposition takes place after the material to be deposited has been transferred to gaseous state either by evaporation or impact process. Chemical methods include the gas phase chemical processes such as conventional Chemical Vapor Deposition (CVD), laser CVD, photo CVD, Metal Organochemical Vapor Deposition (MOCVD) and plasma enhanced CVD. Liquid phase chemical techniques include Electrodeposition, chemical bath deposition, SILAR, electroless deposition, anodization, spray pyrolysis, liquid phase epitaxy etc.

The broad classification of thin films deposition technique is outlined below. Among all these techniques, most of the physical methods are cost expensive; doping is difficult and has following disadvantages.

Splashing causes micron-sized particulates

- Plume highly directional
- Uniform only over a small area
- Mass production hindered
- Extremely complex models eliminates theory based improvements

In chemical methods, spray pyrolysis is simple, cost effective, easy to use, safe, well suited for large area deposition.

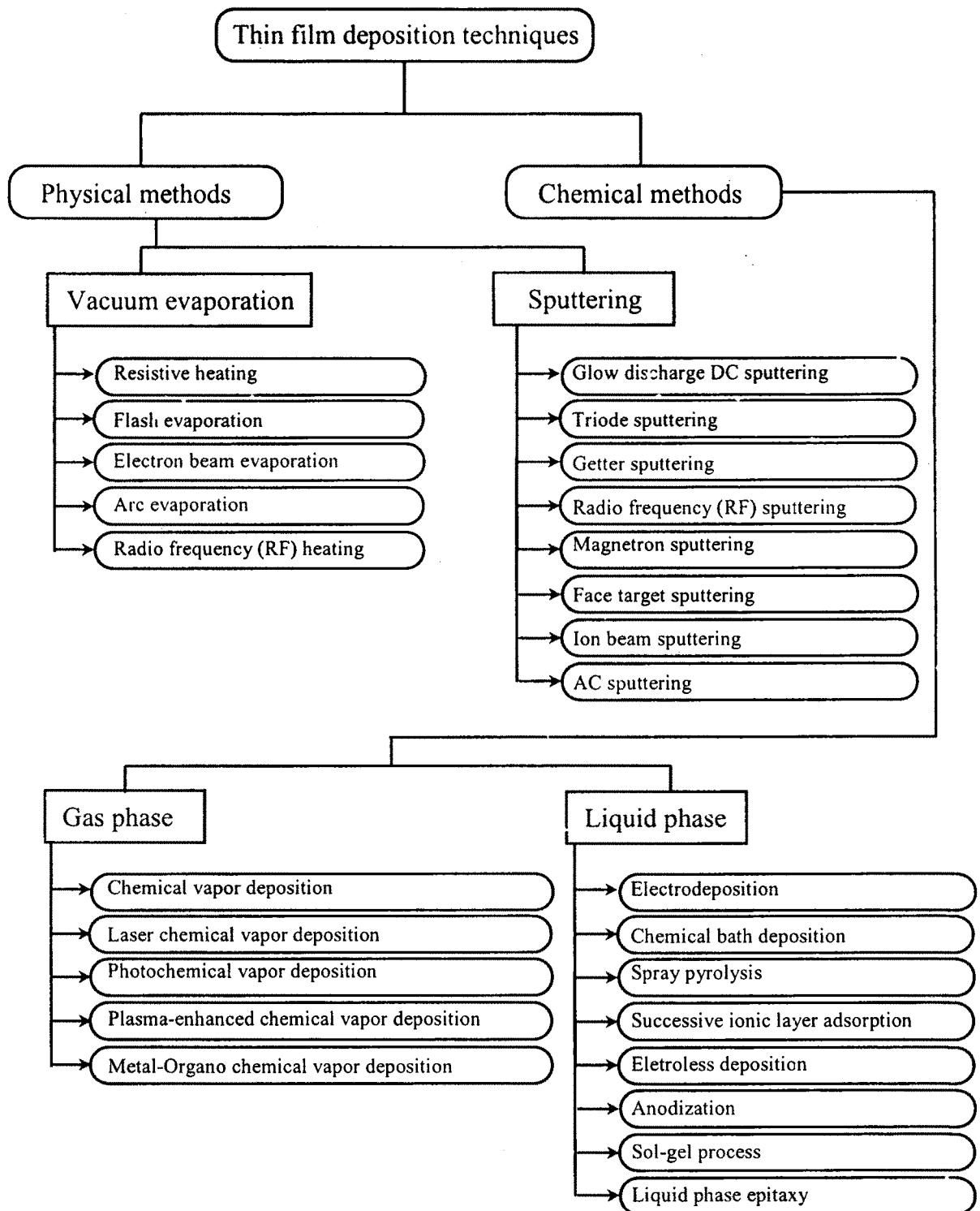


Fig. 2.1 Broad classification of thin film deposition techniques

2.3 Characterization techniques

2.3.1 X-ray diffraction (XRD)

X-ray diffraction is powerful experimental tool used for determination of crystal structure, crystallinity, porosity and lattice parameters, which are based on the interpretation of the X-ray diffraction patterns using Bragg's law [6]. Bragg's law for X-ray diffraction is given by

$$2d \sin \theta = n\lambda \quad (2.1)$$

Where 'd' is interplaner spacing, the 'θ' is the angle of diffraction, 'n' is the integral number and 'λ' is the wavelength of monochromatic X-ray used.

For thin films, the powder diffraction technique in conjunction with diffractometer is most commonly used. Powder diffraction method is first developed by Debye and Scherrer [7] and A. W. Hull [8] independently. The crystal structure analysis can be done by X-ray diffractometer. A movable counter in an X-ray diffractometer replaces Debye Scherrer camera. The diffractometer necessarily uses monochromatic radiations and can be put to investigate single or polycrystalline crystal. As the crystallites are randomly oriented; when X-ray is incident on crystal, a reflection of particular position is due to a set of atomic planes, which satisfy Bragg's condition. In modern X-ray diffractometer, proportional or Scintillation counter is used; which records automatically a graph of intensity of X-rays with respect to Bragg's angle (2θ). In present investigation; X-ray diffraction data of the films are obtained from micro-computer controlled Phillips PW-3710 X-ray diffractometer with Cu-Kα radiation (1.54056 Å). The pattern is taken with zero background intensity using software facility available with the diffractometer.

The X-ray data obtained is compared with JCPDS (Joint Committee for Powder Diffraction Standards) data card of ASTM (American Standards for Testing and Materials) to identify the unknown material. This X-ray diffraction data is used to determine dimensions of unit cell, crystal structure and crystallinity. The grain size of the crystallite is calculated using Scherer's formula [9],

$$D = \frac{k\lambda}{\beta \cdot \cos \theta} \quad (2.2)$$

where k varies from 0.89 to 1.39. But in most of the cases it is closer to 1. Hence for crystallite size calculation it is taken as one, λ is wavelength of X-ray, β is the full width at half of the peak maximum in radians and θ is Bragg's angle.

2.3.2 Scanning electron microscopy

The scanning electron microscope has been widely used for characterization of two dimensional surface topography of thin specimens. All the scanning electron microscopes have facilities for detection of secondary and back scattered electrons. They use incident electron beams with energy between 2-40 KeV. The secondary electrons are orbital electrons knocked out of sample atoms by collisions with incident electron beam. The escape depth of secondary electron is low due to their lower energy (50 eV). Consequently, these electrons are generated at a specimen depth of few nanometers in metal and few tens of nanometer in insulator. The region from they originate is a little than beam diameter. Typical resolution may be order of 5nm [10]. Topographic examinations, the specimens are generally tilted some 20-40 degrees towards the detector in order to get maximum number of secondary electrons. The detector counts the number of secondary electrons produced at its spot, on the surface as electron beam is scanned over specimen surface.

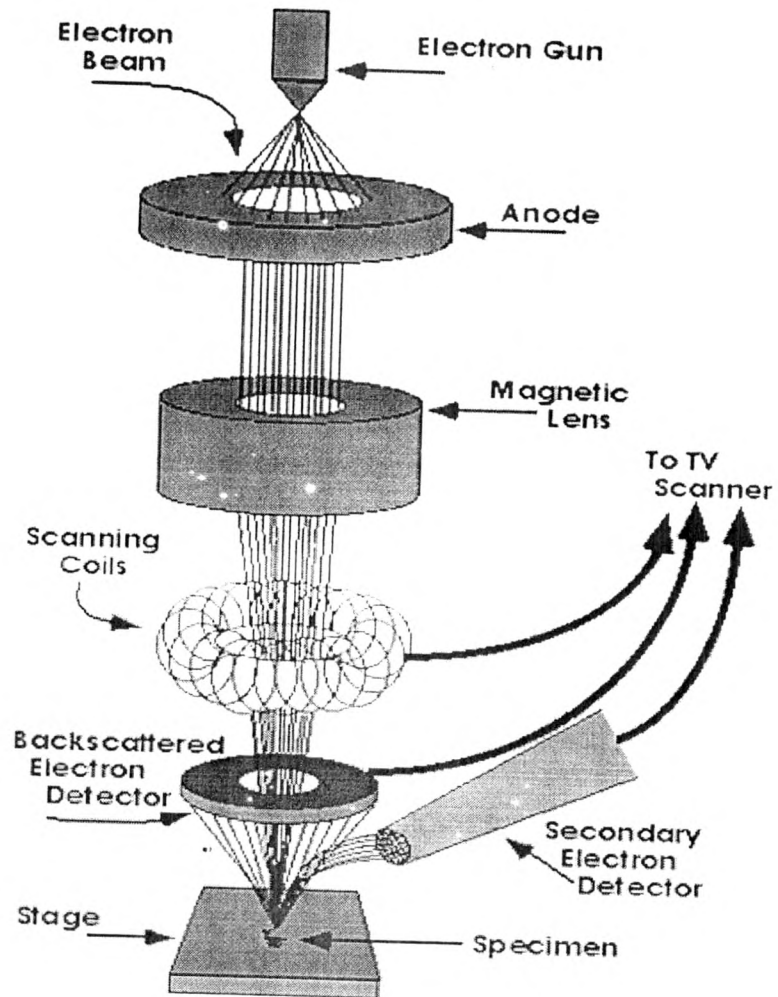


Fig.2.2 Schematic ray diagram of scanning electron microscope 6360

Simultaneously the spot of cathode ray tube is also scanned at the brightness of the spots modulated by amplified current from detector. The overall effect is to produce a topographic image of surface on cathode ray tube screen. Back scattered electrons can be used in scanning electron microscope. When higher energy electrons penetrate into the bulk of specimen, some undergo Rutherford back scattering with atoms and reemerge as back scattered electrons. Thus, the back scattered electron provides information about the bulk (order of 500K). The resolution is poor, however because of spreading of electrons,

this technique is very useful to study the microstructure, grain size, surface morphology etc. One can not obtain the information about interior of sample.

2.3.3 Energy dispersive X-ray analysis (EDAX)

A metal target in an X-ray tube when bombarded with electrons of sufficiently high energy, emit characteristic X-rays. This is the basis of Energy Dispersive X-ray Spectroscopy, a powerful method of chemical analysis of the sample. The EDAX facility is coupled with SEM. The emitted X-rays from the sample bombarded by high-energy electron beam are analyzed in an X-ray spectrometer, and the elements present in the sample are qualitatively identified by their characteristic wavelengths. Quantitative estimation is also possible by measuring relative intensities in the X-ray spectra. For compositions greater than or about 1 % and elements separated by few atomic numbers, EDAX is very useful because the intensities are increased by about 100-fold. Due to limitations of resolution overlapping of lines from nearby elements may occur. The specimen must be either electrically conducting or made so.

2.3.4 Optical absorption and transmission

The equilibrium situation in semiconductors can be disturbed by generation of carriers due to optical photon absorption. Optical photon incident on any material may be reflected, transmitted or absorbed. The absorption of photon will take place when energy of photon ($h\nu$) is greater than the band gap of semiconductor. When the photon energy is less than the band gap energy the incident photon will be transmitted. The intensity of absorbed, transmitted and reflected photons are related by Bouger-Lambert law;

$$\begin{aligned} I_t &= (I_0 - I_r)e^{-\alpha t} \\ I_{abs} &= (I_0 - I_r)(1 - e^{-\alpha t}) \end{aligned} \quad (2.3)$$

where α is coefficient of absorption and t is thickness of sample [11].

The phenomena of radiation absorption in a material is altogether considered to be due to inner cell electrons valence band electrons free carrier including holes as well as electrons and electron bound to localized impurity centers or defects of some type. The first group of electrons does not contribute to either absorption or dispersion in the spectral region with which we are concerned. Absorption by second type of carriers i.e. valence band electrons is of greatest importance in the study of fundamental properties of the semiconductors.

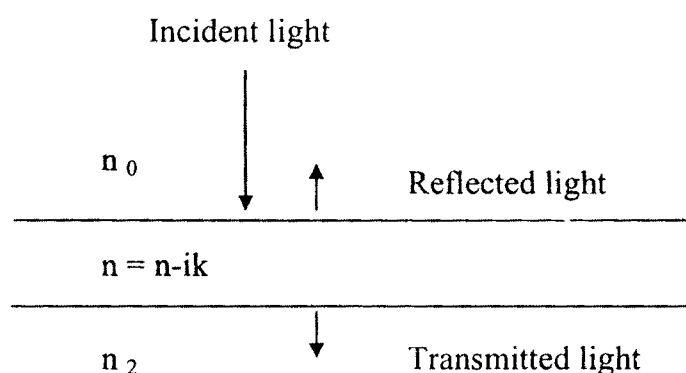


Fig. 2.3 Reflection and Transmission of light by a single film

In ideal semiconductors, at absolute zero temperature the valence band would be completely full of the electrons, so that electron could not be excited to higher energy state from the valence band. Absorption of quanta of sufficient energy i.e. $h\nu > E_g$ tends to transfer of electrons from valence band to conduction band. If the quanta has energy $h\nu < E_g$ then the incident quanta will be transmitted and it will be detected by detector [12]. At first sight determination of amplitudes and intensities of light beams transmitted or reflected by a system of several films is straightforward.

We need to set up the Maxwell's equations and apply boundary conditions. If we consider a wave with angular velocity ' ω ' traveling in the (λ, μ, ν) direction, the electric vector may be written as,

$$E = E_o \exp \left[i\omega \left(t - n \frac{(\lambda x + \mu y + \nu z)}{c} \right) \right] \quad (2.4)$$

where c is the velocity of light in vacuum.

When describing the interaction between light and an absorbing media, we may use the equation of propagation of light in transparent medium, by replacing the refractive index n by a complex quantity of which imaginary part is related to the absorption quantity. The corresponding expression in an absorbing medium will be,

$$E = E_o \exp \left[i\omega \left(t - \frac{\alpha(\lambda x + \mu y + \nu z)}{c} + i\beta \frac{(\lambda x' + \mu y' + \nu z')}{c} \right) \right] \quad (2.5)$$

Where (λ', μ', ν') is the direction of the normal to the planes of equal amplitude.

In this values of α and β depend on the direction of propagation in the medium, and therefore depends on the incident angle. If the angle of incidence is θ and the angle between the planes of constant phase and constant amplitude is ' ϕ ', we may have directly from the wave equations,

$$\begin{aligned} \alpha^2 - \beta^2 &= n^2 - k^2 \\ \alpha\beta \cos\phi &= nk \\ \sin\theta &= \alpha \sin\phi \end{aligned} \quad (2.6)$$

For normal incidence, by considering an electric field part of wave may be written as,

$$E = E_o \exp \left[i\omega \left(t - \frac{(n - ik)(\lambda x + \mu y + \nu z)}{c} \right) \right] \quad (2.7)$$

Where, ' η ' is the ratio of the velocity of wave in vacuum to its velocity in the medium. The energy absorption is represented by k . In order to solve the problem of light reflected and transmitted from boundary separating two materials, we apply boundary conditions to Maxwell's equations. These conditions require that the tangential components of both the electric and magnetic vectors be continuous at the boundary, fig. 2.5

Let us consider a plane wave incident on the surface $z = 0$, the plane of incident being the x - z plane, the angle of incidence ϕ_0 and ϕ_1 . Here there is a use in the assumption that the surface is infinite in extent.

Each wave is constructed from a constant factor and phase factor. The different phase factors associated with the incident and transmitted waves are of the form:

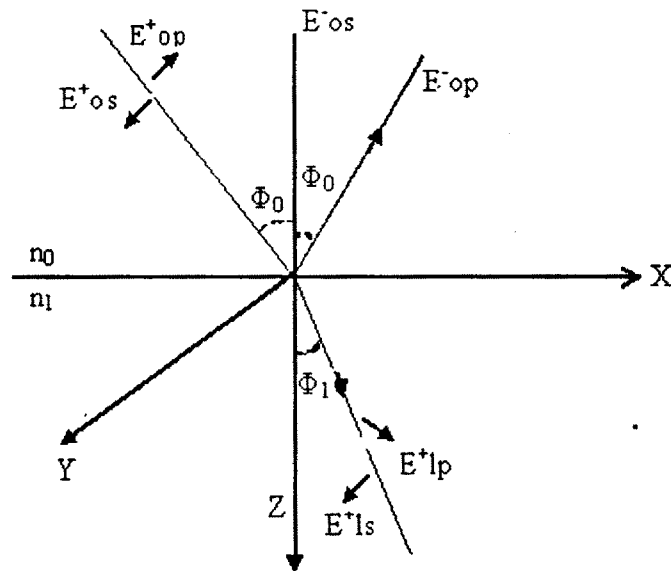


Fig. 2.5 A co-ordinate system of a plane wave incident on a surface

$$\text{Incident- } \exp \left[i \left(\omega t - \frac{2\pi n_0 x \sin \phi_0}{\lambda} - \frac{2\pi n_0 x \cos \phi_0}{\lambda} \right) \right] \quad (2.8 \text{ (a)})$$

$$\text{Transmitted- } \exp \left[i \left(\omega t - \frac{2\pi n_1 x \sin \phi_1}{\lambda} - \frac{2\pi n_1 x \cos \phi_1}{\lambda} \right) \right] \quad (2.8 \text{ (b)})$$

Where, λ is the wavelength in vacuum.

We will write the electric and magnetic total component in the $z = 0$ plane.

For the first medium;

$$\begin{aligned} E_{ox} &= (E^+_{op} + E^-_{op}) \cos \varphi_0 & E_{oy} &= (E^+_{os} + E^-_{os}) \\ H_{ox} &= n_0 (-E^+_{os} + E^-_{os}) \cos \varphi_0 & H_{oy} &= n_0 (E^+_{op} + E^-_{op}) \end{aligned} \quad (2.9)$$

for second medium;

$$\begin{aligned} E_{lx} &= (E^+_{lp}) \cos \varphi_1 & E_{ly} &= (E^-_{ls}) \\ H_{lx} &= -n_1 (E^+_{ls}) \cos \varphi_1 & H_{ly} &= n_1 (E^+_{lp}) \end{aligned} \quad (2.10)$$

by applying the boundary conditions, we can obtain the amplitudes of the transmitted and reflected vectors as the ratios of the incident vectors,

$$r_{lp} = \frac{E^-_{op}}{E^+_{op}} = \frac{n_0 \cos \varphi_0 - n_1 \cos \varphi_0}{n_0 \cos \varphi_0 + n_1 \cos \varphi_0} \quad (2.11)$$

$$t_{lp} = \frac{E^+_{lp}}{E^+_{op}} = \frac{2n_0 \cos \varphi_0}{n_0 \cos \varphi_0 + n_1 \cos \varphi_0} \quad (2.12)$$

$$r_{ls} = \frac{E^-_{rs}}{E^+_{os}} = \frac{n_0 \cos \varphi_0 - n_1 \cos \varphi_1}{n_0 \cos \varphi_0 + n_1 \cos \varphi_1} \quad (2.13)$$

$$t_{ls} = \frac{E^+_{ls}}{E^+_{os}} = \frac{2n_0 \cos \varphi_0}{n_0 \cos \varphi_0 + n_1 \cos \varphi_1} \quad (2.14)$$

Where, r 's are Fresnel's reflection coefficient and Fresnel's transmission reflection coefficient.

For single film

We consider a beam incident on the film, which is divided into reflected and transmitted parts. Such division occurs each time the beam strikes on interface. Summing the multiple reflected and transmitted, we obtain the reflected and transmitted beams.

Let us consider the Fig. 2.6. Suppose that a parallel beam of unit amplitude and of wavelength λ falls on a plane, parallel sided, homogenous, isotropic film of thickness 'd' and refractive index ' n_1 ' supported on a substrate of index ' n_2 '. The index of first medium n_0 and the angle of incidence in this medium is Φ_0 .

Writing δ_1 for the change of phase of the beam on traveling the film, we obtain

$$\delta_1 = \frac{2\pi}{\lambda} n_1 d_1 \cos \phi_1$$

Combining Fresnel's coefficients for reflected amplitude is given by,

$$R = r_1 + t_1 t_1' r_2 e^{-2i\delta_1} - t_1 t_1' r_1 r_2^2 e^{-4i\delta_1} + \dots$$

$$R = r_1 + \frac{t_1 t_1' r_2 e^{-2i\delta_1}}{1 + r_1 r_2 e^{-2i\delta_1}} \quad (2.15)$$

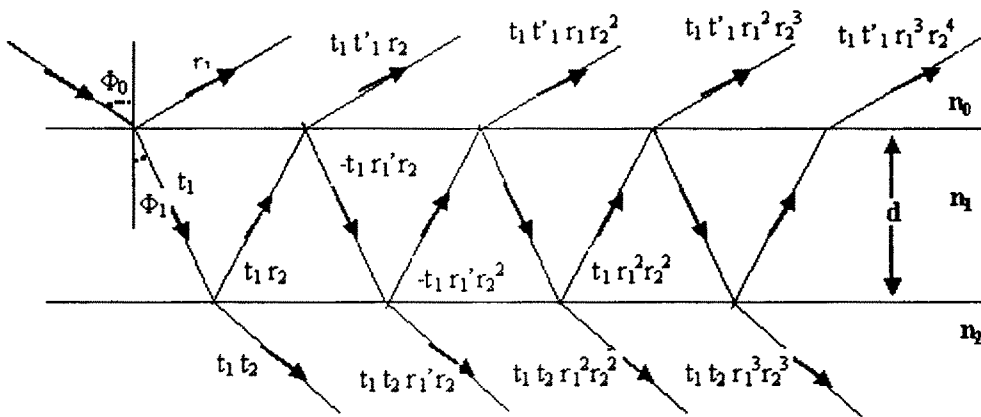


Fig. 2.6A parallel beam of light falls on a plane film supported on a substrate

The transmitted amplitude is given by,

$$T = t_1 t_2 r_2 e^{-i\delta_1} - t_1 t_2 r_1 r_2 e^{-3i\delta_1} + t_1 t_2 r_1^2 r_2^2 e^{-5i\delta_1} - \dots$$

$$T = \frac{t_1 t_2 e^{-i\delta_1}}{1 + r_1 r_2 e^{-2i\delta_1}} \quad (2.16)$$

From the law of the conservation of energy, we can obtain,

$$t_1' = \frac{1-r_1^2}{t_1} \quad (2.17)$$

So the above equations 2.18 and 2.19 becomes

$$R = r_1 + \frac{r_1 + r_2 e^{-2i\delta_1}}{1 + r_1 r_2 e^{-2i\delta_1}} \quad \text{and} \quad T = \frac{t_1 t_2 e^{-i\delta_1}}{1 + r_1 r_2 e^{-2i\delta_1}} \quad (2.18)$$

Equations (2.20) are generally valid for non normal incident each takes two possible forms depending on the state of polarization of incident light. Here R and T represent the amplitudes and in order to receive the energy, we should multiply the square of amplitude with the appropriate refractive index.

$$\text{Energy}_{\text{reflected}} = n_0 R R^* = \frac{n_0 (r_1^2 + 2r_1 r_2 \cos 2\delta_1 + r_2^2)}{(1 + 2r_1 r_2 \cos 2\delta_1 + r_1^2 r_2^2)} \quad (2.19)$$

$$\text{Energy}_{\text{transmitted}} = n_2 T T^* = \frac{n_2 t_1^2 t_2^2}{(1 + 2r_1 r_2 \cos 2\delta_1 + r_1^2 r_2^2)} \quad (2.20)$$

Then the ratios of the transmitted and reflected waves,

$$R = \frac{r_1^2 + 2r_1 r_2 \cos 2\delta_1 + r_2^2}{(1 + 2r_1 r_2 \cos 2\delta_1 + r_1^2 r_2^2)} \quad (2.21)$$

$$T = \frac{t_1^2 t_2^2}{(1 + 2r_1 r_2 \cos 2\delta_1 + r_1^2 r_2^2)} \times \frac{n_2}{n_0} \quad (2.22)$$

From equation 2.11 to 2.14, for normal incidence we can have,

$$r_1 = \frac{n_0 - n_1}{n_0 + n_1}, \quad r_2 = \frac{n_1 - n_2}{n_1 + n_2}, \quad (2.23)$$

$$t_1 = \frac{2n_0}{n_0 + n_1}, \quad t_2 = \frac{2n_1}{n_1 + n_2} \quad \text{and} \quad \delta = \frac{2\pi n_1 d}{\lambda}$$

Where $n_0 = 1$, R.I. of air, n_1 is refractive index of thin film, n_2 the refractive index of the substrate, d the thickness of thin film, R the reflectance, T the Transmittance and λ is wavelength of incident radiation.

By comparing or fitting the observed transmittance data with the calculated data given by equation (2.24), we can search for a pair of thickness and refractive index [13-16].

2.3.5 Electrical resistivity

Resistivity is the inverse of conductivity. The resistivity of semiconductors due to finite charge carrier mobility which results from various scattering mechanisms, of these lattice scattering and impurity scattering is important. Only lattice scattering is dependent on crystallographic orientation. In absence of scattering events carrier would accelerate under influence of an electric field approaching speed of light. In case of dominance of one impurity type is,

$$\rho_n = \frac{1}{q\mu_n N_D} \quad \text{n-type}$$

$$\rho_p = \frac{1}{q\mu_p N_A} \quad \text{p-type}$$

where, μ_n and μ_p are majority's carrier mobilities. N_D and N_A are ionized donors and acceptors.

The semiconductor Resistivity is function of temperature of impurity concentration and of electric field. The conductivity or Resistivity of semiconductor may be locally affected by influences. The carrier concentration is also a function of Fermi level which is temperature dependent. Four distinct temperature ranges are observed in a given semiconductor in which resistivity is affected in different ways by temperature.

References

- [1] Tatsuo Fukano, Tomoyoshi Motohiro, Sol. Energy Mater. Solar Cells 82 (2004) 567.
- [2] Haitema, J.J.Ph, Elich, C.J.Hoogendoorn, Sol. Energy Mater. Solar Cells 18 (1989) 283.
- [3] M.Fantini, Toriani; Thin Solid films 138 (1986) 255.
- [4] K. L. Chopra and I. J. Kaur, Thin Film Devices and Applications, Plenum Press, New York (1983).
- [5] J. George, Preparation of Thin Films, Marcel Dekker, Inc., New York (1963).
- [6] W. L. Bragg, Nature, 95 (1915) 561.
- [7] P. Debye and Scherrer, Physica, 17 (1916) 277.
- [8] A. W. Hull, Phys. Rev., 9 (1916) 504 and ibid, 10 (1917) 661.
- [9] P. Scherrer, Gothinger, Nachri-Chten, 2 (1918) 98.
- [10] D.W.Estrada, D.R.Costa. N.E.Andrade, M.Mikiyoshida, F.Paraguay; Thin solid films 350 (1999) 192.
- [11] Photo electrochemical Solar Cells, Gordon and Breach Science Publishers, New York.
T. M. Moss, "Optical Properties of Semiconductors" O. S. Heavens, Optical properties of Thin Solid Films, Academic Press, (1991).
- [12] Rourard P. Ann. D. Physique, 7 (1937) 291.
- [13] A. W. Crook, I.O.S.A., 38 (1948) 954.
- [14] C. Kittel, Introduction to Solid State Physics, 7th Ed., John Wiley & Sons, Inc., Singapore, New York, (2002).
- [15] C. H. Hall, Amer. J. Math., 2 (1879) 287.
- [16] L. J. van der Pauw, Philips, Res. Repts. 13 (1958) 1.